

Exploiting Simultaneous Multithreading in Priority-Driven Hard Real-Time Systems

Sims Hill Osborne, Shareef Ahmed, Saujas Nandi, and James H. Anderson

Department of Computer Science

University of North Carolina

Chapel Hill, North Carolina, U.S.A.

{shosborn, shareef, saujas, anderson} @cs.unc.edu

Abstract—Simultaneous Multithreading (SMT) has the ability to dramatically improve real-time scheduling, but existing methods are cumbersome, frequently need specialized hardware, or are limited to producing table-based schedules. Here, an easily portable method for quickly applying SMT to priority-driven hard real-time systems is given. Using a combination of integer linear programming and heuristic bin-packing, a partitioned Earliest-Deadline-First (EDF) scheduler that takes advantage of SMT is produced. The integer linear programming and partitioning are done offline, but generally require only a few seconds, even given over a hundred tasks. A large-scale schedulability study is conducted, showing that compared to partitioned scheduling without SMT, the schedulable utilization for the considered hardware platform is nearly doubled in the best cases.

Index Terms—real-time systems, simultaneous multithreading, hard real-time, scheduling algorithms

I. INTRODUCTION

Simultaneous Multithreading (SMT), a technology that allows multiple programs to execute in parallel on a single computing core, is capable of dramatically increasing the ability of a given hardware platform to schedule real-time systems [5, 8, 9, 10, 14, 15, 16, 17]. This benefit can be achieved by taking advantage of SMT’s ability to increase throughput while avoiding situations where increased execution times for individual programs—an inevitable consequence of SMT—cause deadline misses.

Unfortunately, previous work on applying SMT to hard real-time systems requires either purpose-built hardware [16, 17], modifications to basic interactions between the operating system (OS) and hardware [5, 8, 9], or a table-driven schedule [14], which may be undesirable for many applications. In the last case, our own prior work, the methods used to create scheduling tables are time-consuming, thus limiting their applicability to larger systems. These drawbacks limit the industrial applicability of SMT. Even so, industrial users are eager to make use of SMT; in particular, multiple developers have expressed interest to the U.S. Federal Aviation Administration (FAA) in using SMT in safety-critical systems [12].

Work was supported by NSF grants CNS 1563845, CNS 1717589, and CPS 1837337, ARO grant W911NF-17-1-0294, ONR grant N00014-20-1-2698, and funding from General Motors

In this work, we attempt to bridge the gap between the theoretical potential of SMT and applying that potential to an existing system that assumes off-the-shelf hardware and priority-driven scheduling. With that in mind, we show how to use SMT to transform an otherwise unschedulable task system into a task system that can be scheduled using Earliest-Deadline-First (EDF) or another priority-driven scheduler. We do so without sacrificing safety and without relying on a customized hardware platform or OS. As an added bonus to industrial users, we show that our transformation step can be performed quickly—under three seconds, in the majority of scenarios we considered, and in less than a minute for all considered scenarios—so that this stage of testing potential systems will not become a bottleneck in the development process. We judge our methods’ success via a large-scale schedulability study in which we track both the proportion of task systems that can be scheduled on a given platform and how much time is needed to conduct each test.

Contribution and organization. We show within the context of our schedulability study that when we apply our transformation process, the transformed system can be successfully scheduled with partitioned EDF, even, in some cases, when the original system has total utilization approaching double what could be scheduled on the given hardware platform without SMT. Furthermore, the transformation step can be completed in under a minute, even given a system that includes hundreds of tasks. While this may seem like a long time, it is reasonable for a one-time, offline step, particularly considering the possible benefits. The resulting schedule will be no less safe than scheduling the same task system without using SMT.

In Sec. II, we cover necessary background information, including an overview of SMT technology, a review of partitioned EDF scheduling, and an explanation of how we quantify safety. In Sec. III, we give a solution to our problem. The steps of our solution are depicted graphically in Fig. 1. Beginning with an initial task system τ , we use an integer linear program (ILP) to transform it into a system

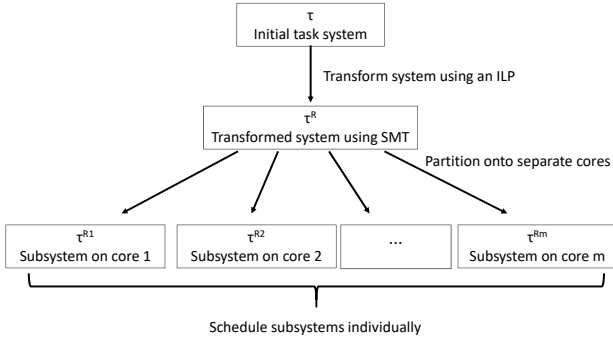


Fig. 1: The steps to achieve partitioned scheduling with SMT.

τ^R that uses SMT¹. The decision to use SMT is made on a per-task basis. This choice is fundamental to the rest of our process, as SMT usage affects many aspects of task behavior. We then partition τ^R into subsystems that are assigned to individual cores, with subsystem $\tau^{R\ell}$ denoting the set of tasks assigned to core π_ℓ . Subsystems on separate cores can then be scheduled using EDF scheduling or another online scheduling algorithm. In Sec. IV, we evaluate our methods via a large-scale schedulability study. In this study, we consider both how large of a task system (in terms of total utilization) can be scheduled on a given hardware platform and how long the transformation step takes. In Sec. V, we conclude and suggest directions for future work.

II. BACKGROUND

In this section, we detail our assumptions regarding our task and hardware platform, provide an overview of SMT technology, and cover key concepts related to partitioned EDF scheduling.

A. Task and Platform Model

We consider the problem of scheduling a periodic hard real-time task system τ that consists of n independent tasks. Each task τ_i releases a single job every T_i time units— T_i gives the task’s *period*—starting at time 0, and each job is assumed to have a maximum cost of $C_i \leq T_i$ time units. We briefly discuss the determination of safe C_i values in Sec. II-C below. The a^{th} job released by τ_i is denoted $\tau_{i,a}$, and tasks are denoted $\tau_i = (C_i, T_i)$. Each task τ_i has a *utilization* given by $u_i = \frac{C_i}{T_i}$. The total utilization of all tasks is given by U . We assume *implicit deadlines*: every job must complete within T_i time units of its release. Our methods work best when the number of distinct periods within τ is small relative to our hardware platform’s core count, but we do not enforce a strict cutoff for the number of different periods.

When SMT is not used for a particular task, every job of that task is fully preemptable; accounting for the costs of

preemption is a well-studied topic. Here, we assume that all task costs are inflated to account for the costs of preemptions without SMT. We assume that interference between jobs executing on separate cores, due to causes including cache conflicts, DRAM conflicts, memory bus conflicts, general OS support, and I/O conflicts, is negligible.² The system is scheduled correctly if it can be shown that no job will ever miss a deadline. An individual task is said to be scheduled correctly if no job of that task will ever miss a deadline. We introduce additional task notation, and discuss how we handle preemptions when SMT is used, as part of our overview of SMT below.

Our hardware platform π consists of m identical computing cores. Each core can support either one job that uses the whole core or two jobs that employ SMT at any given time; these conditions match those of both Intel and AMD processors that support SMT. We refer to tasks whose jobs are scheduled to execute in parallel on a single core as *paired tasks* (formally defined in Def. 3 below). Tasks that do not use SMT are referred to as *solo tasks*.

B. Overview of SMT Technology

On modern computers, each core uses instruction-level parallelism within jobs to execute multiple instructions per cycle. When SMT is enabled, this behavior is expanded to allow multiple jobs to execute instructions within a single cycle. An overview is given in Ex. 1 and Fig. 2 below, both of which closely follow explanations found in our previous work [14]. Further information on the fundamentals of SMT can be found in the works of Eggers et al. [6]. For a detailed discussion of factors that can affect SMT execution in practice, see [2, 3].

Ex. 1. At the top of Fig. 2, jobs of tasks τ_1 (darker colored) and τ_2 (lighter colored) execute sequentially without SMT on a core that can accept two instructions per cycle. When fewer than two instructions are ready, as in cycles 3 and 4, execution resources are wasted. τ_1 finishes at the end of 6 cycles and τ_2 at the end of 12. In the second part of the figure, the same jobs employ SMT to execute in parallel, thereby reducing the number of lost cycles. τ_1 finishes after 8 cycles and τ_2 after 10. SMT thus delays the completion of τ_1 , but speeds up the completion of τ_2 since it does not have to wait for τ_1 to complete before beginning its own execution.

In addition to increasing the execution time of individual jobs, SMT can make it more difficult to predict job execution times due to interactions between jobs that share a core. To mitigate this problem, we require that jobs employing SMT be *simultaneously co-scheduled*.

Def. 1. [14] Two jobs are *simultaneously co-scheduled* if both begin execution simultaneously on separate hardware

²How to limit this interference is an ongoing research topic; our prior work [14] includes references to many papers on this topic.

¹We use the “R” superscript to avoid any confusion with T for time.

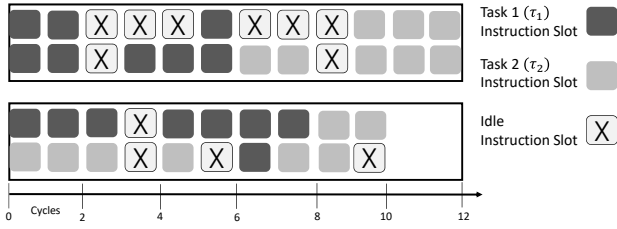


Fig. 2: Top: task execution without SMT.
Bottom: execution with SMT.

threads of the same core, and when one job completes, the remaining job continues on the same core until complete. $\tau_{i.a:j.b}$ denotes the simultaneously co-scheduled jobs $\tau_{i.a}$ and $\tau_{j.b}$. ◀

Simultaneously co-scheduled jobs require their own definitions for execution costs.

Def. 2. [14] The *joint cost* to simultaneously execute jobs of τ_i and τ_j , denoted by $C_{i:j}$, is defined as the execution time for both jobs assuming they begin simultaneously. In Fig. 2, the joint cost of τ_1 and τ_2 is given by $C_{1:2} = 10$. If $i = j$, then $C_{i:i} = C_i$, indicating solo execution for τ_i . Jobs with nothing co-scheduled are *solo jobs*. ◀

We require simultaneous co-scheduling to limit the possibilities we need to consider when determining the execution costs of paired tasks. Without this restriction, we would need to consider in addition to the case of Ex. 1 the time required to execute τ_1 if it began while τ_2 was already executing on the same core, the time required to execute τ_1 if τ_2 began executing later on the same core, and many other possibilities, creating an insurmountable timing-analysis burden.

C. Safety

With or without SMT, safely running a task system requires that stated values for C_i and $C_{i:j}$ accurately reflect the true costs for these items. Determining these values is non-trivial; indeed, finding the true worst-case execution times (WCETs) for tasks on modern, complex processors may be essentially impossible [4]. If a platform includes multiple cores or supports SMT, timing analysis becomes harder still. For this reason, we use measurement-based probabilistic timing analysis (MBPTA) for both solo and paired tasks. The key to producing a safe measurement-based analysis is that execution times need to be measured in circumstances that match their anticipated runtime circumstances. For this reason, we do not allow unrestricted preemptions on tasks that use SMT. If we did allow unrestricted preemptions, our measurements would need to account for all possible ways in which tasks could be preempted, but we are not aware of any existing work that considers how to account for preemption overheads with SMT (we plan to address this topic in future work).

In our model, the stated costs C_i and $C_{i:j}$ are estimates of the true WCETs based on the maximum observed execution time for a given task over many jobs. A task system is, roughly speaking, safe enough if all stated costs C_i and $C_{i:j}$ are such that the probability of the actual cost of an arbitrary job of τ_i or $\tau_{i:j}$ being no more than its stated cost is at least a given value q , where q approaches one. Determining an appropriate value of q is an application-specific decision; further details of this model, including how to determine C_i and $C_{i:j}$ values given a particular q , are covered in [14].

D. Scheduling Tasks using SMT with Partitioned EDF

In this work, we make co-scheduling decisions—our transformation step—at the task level rather than the job level. Doing so creates a much simpler decision process and allows for the use of priority-based scheduling algorithms, such as EDF. To do so, we combine individual tasks into *paired tasks*.

Def. 3. If τ_i and τ_j are *paired tasks*, then the scheduler views $\tau_{i.a}$ and $\tau_{j.a}$ as a single schedulable entity with cost $C_{i:j}$ and relative deadline T_i for all a , i.e., $\tau_{i.a:j.a}$ is simultaneously co-scheduled for all a . We require that two paired tasks share a common period. ◀

To schedule τ across multiple cores, we first determine which tasks should be paired together—we discuss this topic further in Sec. III—and then assign tasks and paired tasks to individual cores. Treating each paired task as a single unit, we then test the tasks assigned to each core for schedulability. We refer to the subset of τ assigned to core π_ℓ as τ^ℓ and say that it has total utilization U^ℓ .

Dealing with preemptions. Safely preempting paired tasks requires careful consideration. The most conservative approach is to make all paired tasks non-preemptable; this is essentially what we did in [14]. However, we can allow more flexibility without introducing undue variation in execution costs by permitting preemption only when SMT is not actually in use. Notice that in Fig. 2, τ_1 finishes before τ_2 . We suspect this scenario to be the typical case; it is unlikely that two jobs will finish at the exact same time. Once the first job has been completed, there is no reason that the remaining job cannot be preempted.

To test for schedulability under the rule that paired tasks are preemptable only at certain times, we need a term for the time during which a task is not preemptable.

Def. 4. Let the *inner cost* of paired task $\tau_{i:j}$, denoted $C'_{i:j}$, give the maximum amount of time during which a job of the paired task $\tau_{i:j}$ is non-preemptable. Typically, this is equivalent to the time required for the first of the paired jobs τ_i and τ_j to complete, although we will discuss other possibilities. For example, in Fig. 2, $C'_{1:2}$ is 8, assuming the pair can be preempted only if one of the two jobs has completed. If we assume that each job of $\tau_{i:j}$ is completely non-preemptable, then $C'_{i:j} = C_{i:j}$. ◀

In terms of schedulability testing, a paired task’s inner cost is equivalent to a non-preemptible section. A uniprocessor EDF schedulability test that accounts for non-preemptible sections within otherwise preemptible tasks is given by Liu in [11].

Def. 5. Let τ_i ’s *blocking term* b_i be the maximum total time for which a job of task τ_i may be prevented from executing by lower-priority jobs. ◀

Theorem 1. [11] *Scheduling τ via EDF on a uniprocessor will result in all deadlines being met if*

$$\sum_{k=1}^n u_k + \frac{b_i}{T_i} \leq 1 \quad (1)$$

holds for all $\tau_i \in \tau$.

If tasks have been partitioned, Exp. (1) can be applied to partitioned EDF by considering only the tasks in τ^ℓ for each core π_ℓ .

When we partition τ^R onto individual cores, we will make use of the following corollary:

Corollary 1. [11] Given task τ_k , b_k is equal to the maximum value of $C'_{i:j}$ for any paired task $\tau_{i:j}$ on the same core for which $T_k < T_i$ holds (recall that for τ_i and τ_j to be paired, $T_i = T_j$ must hold).

Preemption points. If banning preemptions while SMT is in use prevents a task system from being scheduled correctly, we can consider using preemption points. Preemption points are statically inserted into a task’s source code prior to runtime. At runtime, a job that is blocking a higher-priority job will be preempted once a preemption point is reached. The programmer’s challenge in this case is to place preemption points to limit the maximum amount of time for which a job can be non-preemptible, thereby capping b_i in Theorem 1. This topic has been recently addressed by Baruah and Fisher [1]. A similar principle can be applied to paired tasks. With preemption points in place, it is possible to measure execution times between them, allowing for tasks to be preempted at the selected points without compromising safety.

In our schedulability tests (Sec. IV), we consider the effect of placing preemption points so that maximum $C'_{i:j}$ values can be guaranteed. We find that in some cases, particularly when a task system contains many periods, their use can improve schedulability dramatically, but in other cases they make little to no difference.

III. SCHEDULING HEURISTICS

In this section, we describe the full process of scheduling a system with SMT. We do so in three steps; each step is detailed in its own subsection. First, we *transform* our starting task system τ into a new system, τ^R , that employs SMT for some tasks. Second, we *partition* the tasks and paired tasks of τ^R onto individual computing cores. Third,

we *test* each core individually to see if employing EDF on that core will produce a correct schedule. The first two steps are to be done offline, but the scheduling of individual cores is to be done online.

A. Transforming the System

In this subsection we show how to transform τ into an equivalent system τ^R in which some tasks are replaced by paired tasks. “Equivalent” here means that if τ^R is scheduled correctly, then τ is also scheduled correctly. The idea behind using paired tasks is to decrease the total amount of time needed to correctly schedule both of the two tasks within a pair. Since we require that paired tasks share a period, a paired task $\tau_{i:j}$ has the same relative deadline as its component tasks τ_i and τ_j . Consequently, if $\tau_{i:j}$ is scheduled correctly, then τ_i and τ_j are also scheduled correctly. It follows that τ can be correctly scheduled by combining some tasks into pairs and then correctly scheduling all solo tasks and all task pairs, treating each task pair as if it were a single task.

To aid in our explanations, we define a system’s total utilization when task pairs are treated as if they were individual tasks.

Def. 6. The *transformed utilization* U^R of system τ^R is given by

$$\sum_{\forall i: \tau_i \text{ is a solo task}} u_i + \sum_{\forall i, j: i > j, \tau_i \text{ and } \tau_j \text{ are paired}} \frac{C_{i:j}}{T_i}. \quad (2)$$

We use $U^{R\ell}$ for the equivalent term when considering only the tasks and task-pairs assigned to a single core π_ℓ . ◀

When considering if a portion of τ^R is schedulable on a single core, we can safely replace the summation in Exp. (1) with $U^{R\ell}$.

Which tasks should be paired? Given the role that total utilization plays in determining schedulability, it is reasonable to define task pairs so as to minimize total paired utilization. We can do so using an ILP with decision variables $x_{i,j}$ for all tasks τ_i and τ_j within τ .

Def. 7. For all i and all j such that $T_i = T_j$, let $x_{i,j}$ equal 1 if τ_i and τ_j are paired with each other and 0 otherwise. For $i = j$, let $x_{i,j}$ equal 1 if τ_i is a solo task in τ^R and 0 otherwise. Since we do not consider pairing tasks where $T_i \neq T_j$, we define $x_{i,j} = 0$ for those cases. ◀

With Def. 7 in place we can write U^R as follows:

$$\sum_{i=1}^n \sum_{j=i}^n x_{i,j} \cdot \frac{C_{i:j}}{T_i}. \quad (3)$$

Recall from Def. 2 that for solo tasks, we define $C_{i:j} = C_i$; hence for $i = j$, $\frac{C_{i:j}}{T_i} = u_i$.

ILP constraints. In order for τ^R to be equivalent to τ , all tasks within τ must be accounted for in τ^R . To enforce this rule, we require that

$$\forall i \leq n : \sum_{j=1}^n x_{i,j} = 1 \quad (4)$$

holds; essentially, all tasks within τ must appear in τ^R either as a solo task or as part of a paired task.

Additionally, just as τ will be unschedulable if $C_i > T_i$ holds for any task, τ^R will be unschedulable if $C_{i,j} > T_i$ holds for any paired task $\tau_{i,j}$. We therefore require that the following holds:

$$x_{i,j} \cdot C_{i,j} \leq T_i, \quad (5)$$

i.e., τ_i and τ_j may be paired only if $C_{i,j} \leq T_i$ holds. Since we require that only tasks sharing a period may be paired, we do not need a separate restriction governing the relative values of $C_{i,j}$ and T_j .

Finally, note that Def. 7 actually defines both $x_{i,j}$ and $x_{j,i}$ for each possible task pair. To avoid any inconsistencies, we add the restriction that

$$\forall i, j : x_{i,j} = x_{j,i}. \quad (6)$$

We define our ILP as minimizing Exp. (3) subject to Exps. (4) through (6). Despite using integer variables, our ILP executed reasonably quickly in the experiments presented in Sec. IV. We discuss execution times in more detail in Sec. IV.

B. Partitioning the Transformed System

After defining τ^R , our next step is to partition it onto the individual cores of π . Even without considering non-preemptive sections, assigning tasks and task pairs to cores so that all cores are schedulable is a bin-packing problem. While bin-packing is NP-complete in the strong sense, multiple well-studied approximation algorithms for it exist. We use two of these algorithms—worst-fit decreasing and best-fit decreasing bin-packing—and two algorithm variations of our own, giving us a total of four partitioning algorithms. After assigning tasks to cores, schedulability is tested per Theorem 1 and Corollary 1. In all cases, we assign tasks to cores in non-increasing order of $\frac{C_{i,j}}{T_i}$ and view each core as a single bin with capacity 1.0.

Worst-fit decreasing and best-fit decreasing. In worst-fit bin packing, each task or paired task is placed on the core that will maximize remaining capacity on the selected core. In best-fit bin packing, each task or paired task is placed on the core that will minimize remaining capacity on the selected core.

Period-aware bin-packing. In our second two algorithms, we modify the worst-fit and best-fit algorithms in an attempt to limit the number of different periods on any one core; note that one consequence of Corollary 1 is that

if all tasks on a given core share the same period, then no task is subject to priority-inversion blocking. In this case, the core is schedulable if and only if $U^{R\ell} \leq 1$ holds.

In *period-aware worst-fit partitioning*, we again attempt to place tasks and task-pairs on cores in non-increasing order of $\frac{C_{i,j}}{T_i}$. In this method, we potentially make two attempts to assign each task to a core. In the first attempt, we use worst-fit bin-packing to assign a task or paired task to a core, but we consider only cores on which all previously assigned tasks have the same period as the current task. If a task or paired task is assigned to a core at this point, we move on to the next task or paired task. If the task or pair cannot be placed onto a core using this method, we consider all cores of the platform and assign the task using the standard worst-fit decision process.

Period-aware best-fit partitioning is similar—we first attempt to schedule each task considering only cores without any different periods—but using best-fit rather than worst-fit bin-packing to determine the assignments of tasks to cores.

C. Testing Individual Cores

Our final step is to test each core for schedulability using Theorem 1. To do so, we treat each paired task as if it were a single task. After tasks have been partitioned, the process is no different from uniprocessor scheduling without SMT. While we use EDF in this paper, there is no reason why another uniprocessor scheduling algorithm, such as rate-monotonic (RM) scheduling, cannot be used; the only change needed to use a different per-core scheduling algorithm would be to use a different schedulability test than that of Theorem 1.

IV. EXPERIMENTS

In this section, we present our experimental results. To evaluate our scheduling methods, we conducted a schedulability study in which we created tens of thousands of synthetic tasks across nearly 2,000 scheduling scenarios. For each scenario, we compared the effectiveness of scheduling task systems using our ILP combined with our four bin-packing algorithms—worst-fit, best-fit, period-aware worst-fit, and period-aware best-fit—against scheduling the same systems without SMT. In the last case, our baseline, scheduling is attempted using partitioned EDF, with worst-fit decreasing bin-packing as the partitioning algorithm.

A. Experimental Setup

We examined 1,728 scenarios, with each scenario defined by a core count, per-task utilization range, period set, SMT interaction model, and an inner cost model.

The first three factors of our scenario definition require only a brief explanation. The last two are covered in more detail below. We considered core counts of four, eight, and sixteen. Solo per-task utilizations were drawn from

four uniform ranges: (0, 0.4) (*low*), (0.3, 0.7) (*medium*), (0.6, 1) (*high*), or (0, 1) (*wide*). Periods were drawn from either the set {20, 40, 60, 80, 100} (*five periods*) or the set {10, 20, 30, 40, 50, 60, 70, 80, 90, 100} (*ten periods*).

Each task was created by selecting a utilization from the appropriate distribution and a period from the appropriate set, with all periods within a set having equal probability. Periods and utilizations were selected independently. A solo task execution cost was then assigned as a function of utilization and period. For each scenario, we determined schedulability ratios (i.e., the percentage of schedulable task sets) for task systems ranging in total utilization from $\frac{m}{2}$ to $2m$ —recall that m denotes the core count—using each of our four bin-packing algorithms to partition τ^R onto separate cores after having transformed τ into τ^R using our ILP. We compared these results to a baseline of schedulability ratios found without SMT using partitioned EDF, with partitioning determined by decreasing worst-fit bin-packing.

In order for our study to be useful, we need to model realistic relationships between values for C_i , C_j , $C_{i;j}$, and $C'_{i;j}$. To do so, we used benchmark data we presented in our prior work [14], where we compared worst-observed execution times with and without SMT for programs selected from the TACLeBench sequential benchmarks, which is representative of real-world embedded and real-time workloads [7].

Modeling $C_{i;j}$. Previously [14], we modeled $C_{i;j}$ by defining a *multithreading score*, which determines $C_{i;j}$ given C_i and C_j . We repeat that definition here.

Def. 8. [14] If $\tau_{i;j}$ is a task pair for which $C_i \geq C_j$ holds, then the *multithreading score* $M_{i;j}$ satisfies the following:

$$C_{i;j} = C_i + M_{i;j} \cdot C_j. \blacktriangleleft$$

If $M_{i;j} \geq 1$ holds, then there is no benefit to pairing τ_i and τ_j together. If $M_{i;j} < 1$ holds, then pairing jobs of the two tasks is potentially beneficial, with lower values indicating greater benefit.

In [14], We found that $M_{i;j} > 1$ was frequently the case when C_i and C_j differed by a factor of 10 or more. For this reason, we do not permit tasks with solo costs differing by a factor of 10 or more to be paired. For tasks whose solo execution costs were within a factor of 10, we found that most $M_{i;j}$ values fell between 0.1 and 0.8. These results are summarized in Fig. 3. As in [14], we determined the $M_{i;j}$ values of our synthetic tasks by giving each pair either a 0.0, 0.1, or 0.2 probability of having $M_{i;j} \geq 1$. We refer to this value as the *split*, i.e., a split of 0.1 indicates that each task pair has a 10% chance of being declared unsuitable for SMT. If a task pair was not selected to have $M_{i;j} \geq 1$, then we determined its $M_{i;j}$ value based on one of three normal distributions—(0.45, 0.12), (0.6, 0.07), or (0.45, .06)—or one of three uniform

Fig. 3: Histogram showing the distribution of $M_{i;j}$ values for pairs where $C_i \leq 10 \cdot C_j$. Based on data from [14].

distributions—(0.1, 0.8), (0.4, 0.8), or (0.27, 0.63). All of the normal distributions were truncated, with any negative value produced replaced by 0.01. Further discussion on the data and reasoning behind these values is given in [14].

Modeling $C'_{i;j}$. The $C'_{i;j}$ parameter is original to our present work. Here we consider five methods, presented below, of modeling its relationship to our other cost parameters, C_i , C_j , and $C_{i;j}$. Note that values for $C'_{i;j}$ have no impact on the transformation and partitioning steps of our process; they are only used to test per-core schedulability, after SMT usage has been determined and tasks have been partitioned among individual cores.

No preemption. In this model, our first and most pessimistic, we assumed that $C'_{i;j} = C_{i;j}$, i.e., every paired task is non-preemptable. While this assumption is conservative, particularly when C_i is much greater than C_j , testing schedulability under this condition allowed us to be confident we have considered the true worst-case scenario. It also is essentially what we assumed in [14], allowing us to make a comparison between the process used here and in [14]. The latter can potentially schedule systems with greater total utilization than can be done with the current approach—largely due to deciding when to use SMT on a per-job rather than per-task basis—but is limited to table-based scheduling and may require prohibitively large amounts of time to compute a scheduling table.

Double cost. In this model, we defined $C'_{i;j}$ as the time during which both jobs are executing and then assumed that $C'_{i;j} = \min(C_{i;j}, 2 \cdot C_j)$, with τ_j being the task with the shorter solo cost. This model is still quite conservative; we found our data from [14] shows only one paired task in which $C'_{i;j} > 2 \cdot C_j$ held after excluding tasks for which C_i and C_j differ by more than a factor of 10. Other works [2, 3, 10, 15] have also found that it is rare for execution times to double in the presence of SMT.

Data driven. In this model, we used the same definition of $C'_{i;j}$ as in the double cost model, but rather than assuming that $C'_{i;j} = \min(C_{i;j}, 2 \cdot C_j)$, we based our $C'_{i;j}$ values on how much time was actually required in [14] for the faster-executing job of each pair to finish, with minimal added conservatism. Again excluding cases where C_i and C_j differed by more than a factor of 10, we found that in the majority of cases, the execution time of τ_j alone within the pair $\tau_{i;j}$ —i.e. $C'_{i;j}$ under this model—ranged from slightly greater than C_j to $1.8 \cdot C_j$. There was one outlier for which we had $C'_{i;j} \approx 10 \cdot C_j$.³ This data is shown graphically in Fig. 4.

³This value occurred with a benchmark, petrinet, that is extremely short and was often difficult to measure.

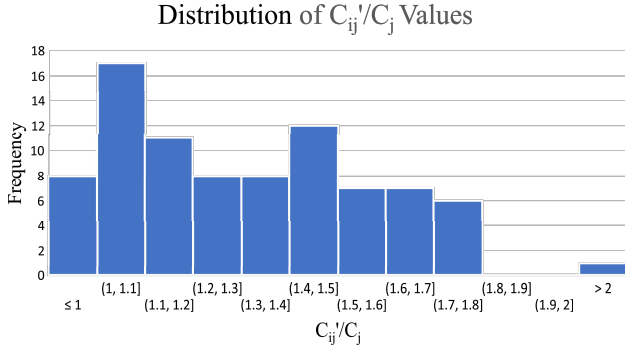


Fig. 4: Histogram showing the distribution of $\frac{\text{time SMT is in use}}{\text{solo execution time of shorter job}}$, i.e. $\frac{C'_{i:j}}{C_j}$, when using the definitions in our data driven model. Based on data from [14].

With that in mind, we gave each potential paired task in this model a 2% chance that $C'_{i:j} = \min(10 \cdot C_j, C_{i:j})$. This step allows for the possibility of $\frac{C'_{i:j}}{C_j}$ being as great as the maximum relative to C_j , $10 \cdot C_j$, that we observed in practice. 2% overstates our observed frequency of this occurrence; our outlier was a single sample out of 84 possibilities. Apart from that possibility, we set each $C'_{i:j}$ value as a uniform random variable in the range $[1.1 \cdot C_j, \min(1.8 \cdot C_j, C_{i:j})]$. Some pessimism persists in this model, as our observed $C'_{i:j}$ values can be seen in Fig. 4 to skew towards the lower end of that range and we do not allow the possibility in our model of $C'_{i:j} < 1.1 \cdot C_j$ holding despite having observed that possibility in practice.

It is noteworthy that in some of our collected data, $C'_{i:j} < C_j$ holds, meaning that in some cases, a job requires less time to complete with SMT than without. At present, we do not have a good explanation for this behavior, and so we pessimistically exclude it from our modeling. We intend to investigate this phenomenon in future work.

Preemption points. In this model, we attempted to capture the effects of allowing preemption points within a task system. In our preemption points model, we assumed that any code we execute has preemption points inserted so that no job will be non-preemptable for more than 10 time units. In this case, we defined $C'_{i:j}$ as the minimum of 10 and what it would have been under the data driven model. We chose 10 with the idea that if each time unit corresponds to one millisecond, placing preemption points to limit non-preemptable sections to 10 ms should be achievable without causing exceptionally high overheads.

Full preemption. Here we assumed that all tasks are fully preemptable, even when there are paired jobs running at the same time. In practice, allowing unrestricted preemptions along with SMT would tend to make the already difficult timing-analysis problem discussed in [14] even harder, possibly making it impossible to guarantee a safe timing analysis for hard-real tasks. However, testing

this approach allowed us to see the cost of limiting preemptions. In addition, this approach may be viable for soft real-time and non-safety-critical systems, where some additional uncertainty in timing analysis may be tolerable.

B. Schedulability Results

To determine whether a task system was schedulable, we attempted to transform⁴ and partition each system created so that the resulting sub-systems were all schedulable on their assigned cores per Theorem 1.

For each scenario considered, we summarize our results in a graph that shows the schedulability ratio of systems ranging in total utilization from $\frac{3m}{4}$ to $2m$, with each point on the graph corresponding to approximately 100 systems.⁵ For each scenario, we show only the partitioning algorithm that produced the best results. Since the partitioning algorithms all execute quickly, it is entirely practical to run all four for each task system and then choose the best result.

We use two metrics to summarize the proportion of systems that are schedulable under each scenario. We define *relative schedulable area* (RSA) as the area under the schedulability curve divided by the core count m for each scenario. In calculating RSAs, we assumed that the schedulability ratio is constant between total utilization 0.0 and $\frac{m}{2}$, which is the smallest utilization we tested in each scenario. This assumption results in RSAs being somewhat understated in the lowest-performing scenarios. An ideal (e.g., fluid) scheduler, not using SMT, that can preempt and migrate jobs arbitrarily would have an RSA of 1.0; it could schedule all task systems with total utilization at most m and no task systems with greater utilization.

In addition to RSA, we define a scenario's *partitioned improvement* (PI) as the RSA for a given scenario and partitioning algorithm divided by the RSA for that same scenario using our baseline scheduling algorithm. We use PI to show the benefit of our methods in cases where partitioned scheduling without SMT falls well short of an ideal scheduler to begin with; for example, the scenario shown in Fig. 13 has an RSA of 0.93. Based on that statistic alone, one might include that SMT is not effective in this case. However, the scenario has a PI of 1.11 showing an improvement over partitioned scheduling without SMT.

Our full set of graphs is included in an online appendix [13]. Here, we show the graphs that give the best, worst, and median results for both RSA and PI when using the full-preemption and data-driven models. These graphs demonstrate several trends we saw in our results.

⁴We used Gurobi Optimizer, a commercial optimization programming solver with free academic licensing, to execute the required ILP.

⁵While we calculated schedulability for utilizations in the range $[\frac{m}{2}, 2m]$, our graphs only show results in the range $[\frac{3m}{4}, 2m]$; in the majority of cases, we found that all systems with utilization less than $\frac{3m}{4}$ could be scheduled.

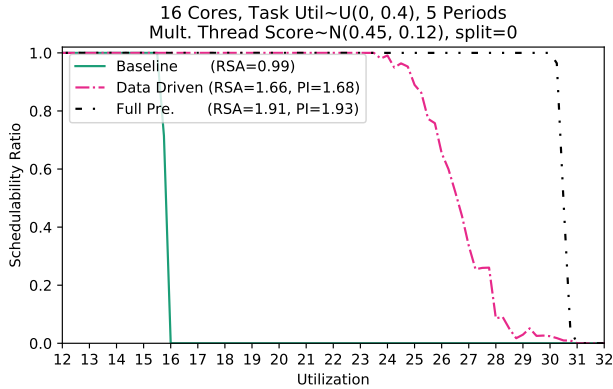


Fig. 5: The best RSA and PI in the full preemptions model and the best RSA in the data driven model.

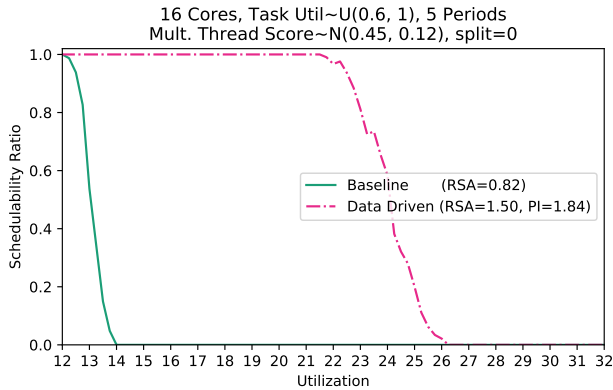


Fig. 6: The best PI in the data driven model.

In some cases, we found that two or more different inner cost models produced near-identical results. Graphically, this result produced graphs that were difficult to read. To avoid this problem, we do not print lines for inner cost models that had the same RSA within two significant digits as the data-driven model.

Obs. 1. With the full preemption model, applying SMT always gave an improvement compared to partitioned EDF, and, in the best cases, nearly doubled schedulable utilization. RSAs ranged from a high of 1.91 (Fig. 5 to a low of 0.83 (Fig. 7) and PIs from a high of 1.93 (Fig. 5 to a low of 1.01 (Fig. 8).

Obs. 2. With the data driven model, applying SMT improved schedulability in more than half of all scenarios, as shown by the median PI of 1.11 (Fig. 13). In the best data driven case, RSA equaled 1.66 (Fig. 5) and PI 1.84 (Fig. 6).

Obs. 3. Applying SMT did not always improve schedulability when using the data-driven model, as shown in Fig. 9. The worst results for models other than full preemption typically occurred when the period count was greater than the core count, as seen in Fig. 9. In these cases, the problem is that the ILP creates a task system that can be scheduled only by allowing more task preemption

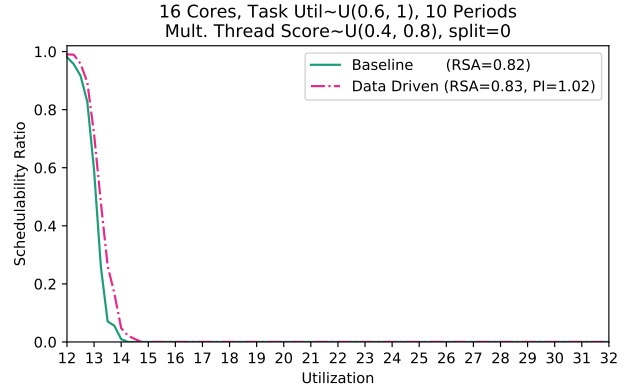


Fig. 7: The worst RSA in the full preemption model

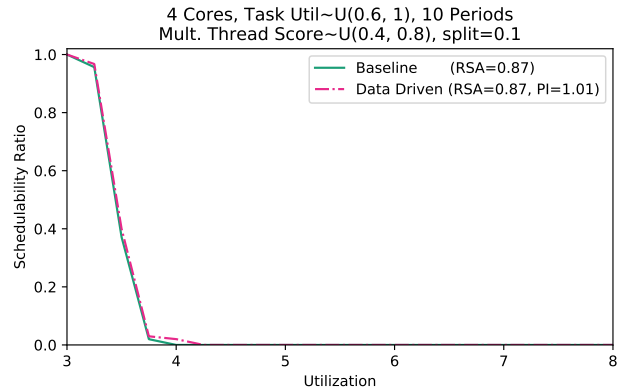


Fig. 8: The worst PI in the full preemption model

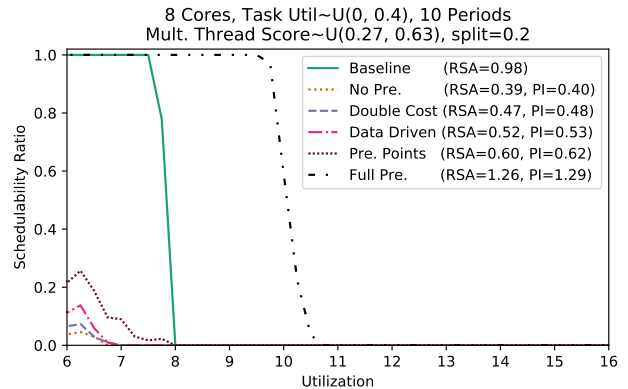


Fig. 9: The worst RSA and worst PI in the data driven model

than we permit; recall that the ILP does not consider inner costs, and that its only restriction on per-task costs is that $C_{i,j} \leq T_i$ must hold.

Obs. 4. The impact of which preemption model is used on overall schedulability varies greatly. In some scenarios, such as that of Fig. 8, it makes essentially no difference, whereas in others, such as Fig. 9, the difference is dramatic. This result suggests that in some cases, further work on means to allow more preemptions of SMT-enabled tasks

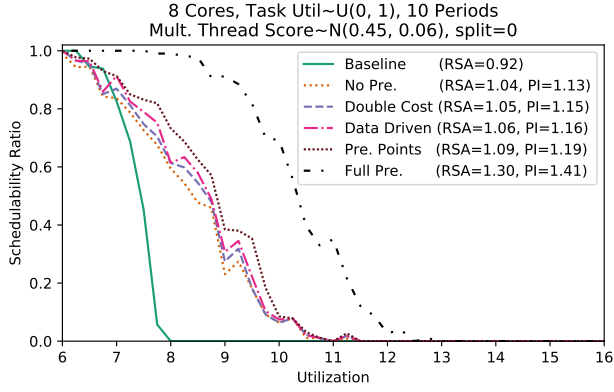


Fig. 10: Median RSA in the full preemption model.

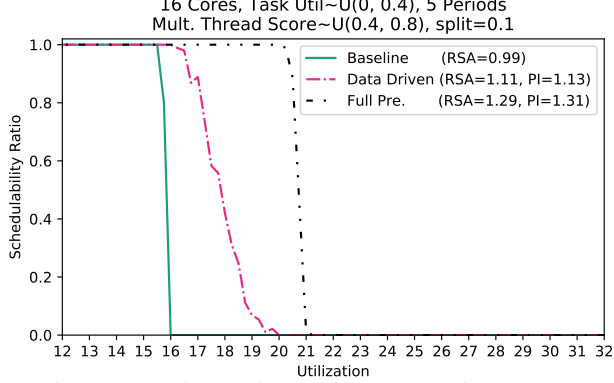


Fig. 11: Median PI in the full preemption model.

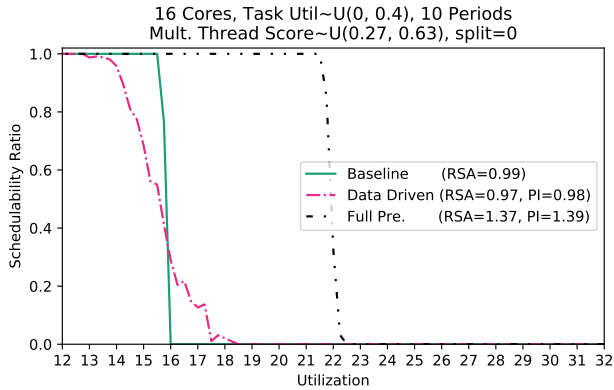


Fig. 12: Median RSA in the data driven model.

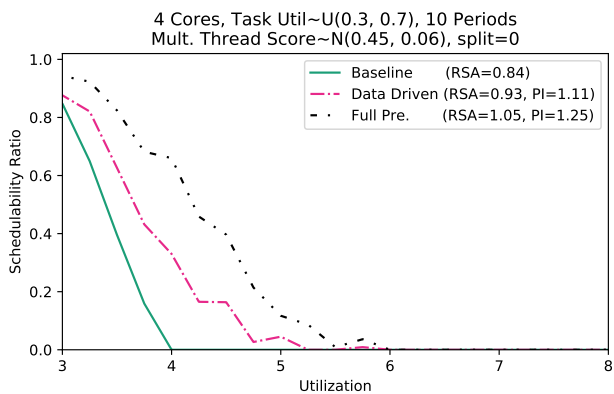


Fig. 13: Median PI in the data driven model.

TABLE I: Period-aware advantages (Def. 9)

Inner cost model	Period-aware advantage
No Preemption	0.75
Double Cost	0.75
Data Driven	0.74
Preemption Points	0.21
Full Preemption	0.01

would be time well spent.

Obs. 5. The period-aware algorithms provided a large advantage under the no-preemption, double-cost, and data-driven preemption models, but were less advantageous using the preemption points and full preemption models. We summarize our findings on the *period-aware advantage* (defined below) of each model in Table I.

Def. 9. For each inner cost model, we define its *period-aware advantage* as the proportion of scenarios in which at least one of the period-aware partitioning algorithms gave a strictly greater RSA than both the best-fit and worst-fit algorithms.

Obs. 6. In no case did our ILP require more than 37 seconds to execute, and only one required more than 30 seconds. The median time required was 2.54 seconds. No four-core system required more than 9 seconds, and no 8-core system required more than 24 seconds. In contrast, ILP execution times of 60 seconds were frequently insufficient in our previous work [14], even on systems of only four cores.

Execution times are summarized in Fig. 14. For each scenario, we recorded only the maximum time required by any ILP, meaning that our discussion here overstates the typical execution time needed. Note that since we considered preemption only after partitioning tasks, each ILP provided data for all five of our preemption models. In total we recorded 432 execution times. Our schedulability tests were performed on a research cluster consisting of 2.5 and 2.3 GHz cores, with tests for many scenarios running in parallel. We suspect that individual ILPs ran significantly slower than they would have had our experiments not run in parallel.

As to whether our ILP execution-time requirements are practical, less than 1 minute is certainly reasonable for an offline step, since that will only be done once per system. Our shortest times—the fastest 5% of our ILPs required less than 100 ms to run—could even be practical to run online as part of a task system allowing dynamic task entry and exit.

V. CONCLUSION

Within the context of our schedulability study, we found that when allowing tasks to be preemptible, schedulability was increased by a factor of 1.5 or more in 31% of tested scenarios. The same improvement was seen in 13% of

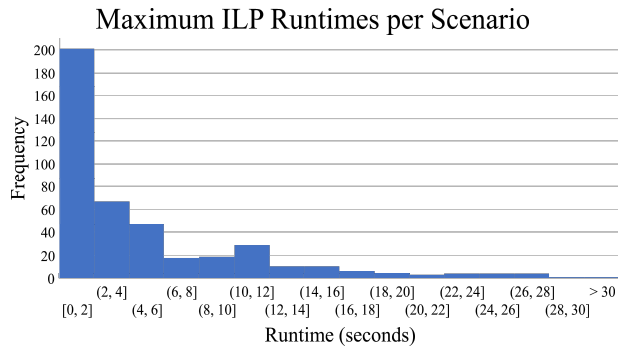


Fig. 14: Histogram showing the distribution of maximum ILP runtimes for each scenario.

scenarios using either data driven inner costs or allowing no preemption at all. Furthermore, we saw schedulability improvements of 1.8 or more in 11% of scenarios that allowed full preemption and in 2% of scenarios using either the data driven or no preemption models.

In future work, we plan to investigate the effects of allowing preemption while SMT is active; by doing so, we hope to enable results that are close to those of our somewhat idealized full-preemption model. If we find that preemptions have a significant detrimental effect on SMT-enabled execution, we will need to rely more on the ability of our period-aware partitioning algorithms to obviate the need for preemptions. Even in systems without SMT, period-aware partitioning may be a useful tool to reduce the need for preemptions; in practice, though we do not model it here, increasing preemptions in a system may come at a cost of reduced schedulability. If that cost can be avoided, so much the better.

The process we have given here may also be suitable for dynamic systems, in which tasks can enter and leave a system during run-time. Given that our transformation step and partitioning algorithms both execute quickly, it may be possible to execute them periodically as scheduled jobs in a live system, with the goal of rebalancing a system whose task mix has changed. For this to be practical, we would need to be able to guarantee run-times for the currently offline portions of our algorithm. In addition, we intend to integrate our work on SMT into a mixed-criticality context.

REFERENCES

- [1] S. Baruah and N. Fisher. Choosing preemption points to minimize typical running times. In *Proceedings of the 27th International Conference on Real-Time Networks and Systems, RTNS '19*, page 198–208, New York, NY, USA, 2019. Association for Computing Machinery.
- [2] J. Bulpin. *Operating system support for simultaneous multithreaded processors*. PhD thesis, University of Cambridge, King's College, 2005.
- [3] J. Bulpin and I. Pratt. Multiprogramming performance of the Pentium 4 with hyperthreading. In *Third Annual Workshop on Duplicating, Deconstruction and Debunking*, pages 53–62, June 2004.

- [4] A. Burns and S. Edgar. Predicting computation time for advanced processor architectures. In *ECRTS 2000*, pages 89–96, Feb. 2000.
- [5] F. J. Cazorla, P. M. W. Knijnenburg, R. Sakellariou, E. Fernandez, A. Ramirez, and M. Valero. Predictable performance in SMT processors: synergy between the OS and SMTs. *IEEE Transactions on Computers*, 55(7):785–799, July 2006.
- [6] S. J. Eggers, J. S. Emer, H. M. Levy, J. L. Lo, R. L. Stamm, and D. M. Tullsen. Simultaneous multithreading: a platform for next-generation processors. *IEEE Micro*, 17(5):12–19, Sept 1997.
- [7] H. Falk, S. Altmeyer, P. Hellinckx, B. Lisper, W. Puffitsch, C. Rochange, M. Schoeberl, R. B. Sørensen, P. Wägemann, and S. Wegener. TACLeBench: A Benchmark Collection to Support Worst-Case Execution Time Research. In *WCET 2016*, pages 2:1–2:10, 2016.
- [8] T. Gomes, P. Garcia, S. Pinto, J. Monteiro, and A. Tavares. Bringing hardware multithreading to the real-time domain. *IEEE Embedded Systems Letters*, 8(1):2–5, March 2016.
- [9] T. Gomes, S. Pinto, P. Garcia, and A. Tavares. RT-SHADOWS: Real-time system hardware for agnostic and deterministic OSes within softcore. In *ETFA 2015*, pages 1–4, Sept 2015.
- [10] R. Jain, C. J. Hughes, and S. V. Adve. Soft real-time scheduling on simultaneous multithreaded processors. In *RTSS 2002*, pages 134–145. Institute of Electrical and Electronics Engineers Inc., 2002.
- [11] J.W.S. Liu. *Real-Time Systems*. Prentice Hall, 2000.
- [12] B. Ocker. FAA special topics. In *Collaborative Workshop: Solutions for Certification of Multicore Processors*, Nov. 2018.
- [13] S. Osborne, S. Ahmed, S. Nandi, and J. H. Anderson. Exploiting simultaneous multithreading in priority-driven hard real-time systems (longer version with additional material), 2020.
- [14] S. Osborne and J. H. Anderson. Simultaneous multithreading and hard real time: Can it be safe? (in submission). 2020.
- [15] S. Osborne, J. Bakita, and J. H. Anderson. Simultaneous multithreading applied to real time. In *ECRTS 2019*, 2019.
- [16] K. Suito, K. Fujii, H. Matsutani, and N. Yamasaki. Dependable responsive multithreaded processor for distributed real-time systems. In *2012 IEEE COOL Chips XV*, pages 1–3, April 2012.
- [17] M. Zimmer, D. Broman, C. Shaver, and E. A. Lee. FlexPRET: A processor platform for mixed-criticality systems. In *RTAS 2014*, pages 101–110, April 2014.